

Making Gabor Noise Fast and Normalized

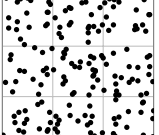
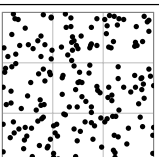
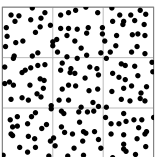
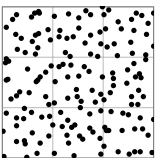
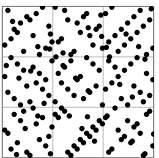
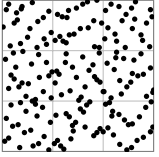
Supplemental material

V. Tavernier, F. Neyret, R. Vergne and J. Thollot

In this supplemental document we provide details about the point distributions used, as well as formulas and justifications about the Cramer von Mises (CvM) criterion, and more precisions about stationarity measures. In figures 3 and 6 we decompose and complete the plots corresponding to figures 2, 3 and 4 in the paper, and in figures 4, 5 and 7 we provide examples of failing criterion when applied on more exotic configurations than the one benched in the paper (like, using no weighting at all).

2. Gabor noise alternative ingredients

Point distribution

Point distribution	Description
	Seminal homogeneous Poisson point process. The process is entirely defined by its (constant) density of impulses per area. In cell-based implementations (more efficient for procedural textures) the density per cell must first be determined using the Poisson law. This point process has a tendency to generate voids and clusters of impulses randomly, <i>i.e.</i> the actual impulse density is probabilistic with some variance around the expected density value given as a parameter.
	Stratified Poisson point process. Instead of sampling the Poisson law to obtain the number of impulses in a given cell, that number is directly set to a constant N corresponding to the target density. Point coordinates are then sampled uniformly in the cell. The density variance is slightly biased along cell edges due to the number of impulses per cell being a constant.
	Rectangular jittered grid point process. As in stratified Poisson, the number of points in a cell is a constant N . Here, each of these N points are then distributed among N sub-cells in which coordinates are sampled uniformly. This spreads out the variance bias present around cell edges in stratified Poisson, thus reducing its amount.
	Hexagonal jittered grid point process. Each of the rectangular sub-cells of the rectangular jittered point process are replaced by two triangular sub-cells, forming an hexagonal tiling. Point coordinates are sampled uniformly over the sub-cell space, taking into account the triangular shape of sub-cells. The hexagonal tiling has more preferred directions than rectangular jittered (3 instead of 2) which results in directional artifacts being less pronounced.
	Sobol [Sob67] point distribution. Point coordinates in cells are obtained using Sobol sequences of varying direction vectors.
	Scrambled Sobol [CBEM05] point distribution. Point coordinates in cells are obtained using scrambled Sobol sequences.

Weights

Our experiments revealed that the use of Bernoulli weighting allows for much faster convergence of the noise process than the uniform one. Aside from the metrics attesting this increased convergence speed at matching quality, we did not notice any artifacts due to this change, see fig. 1.

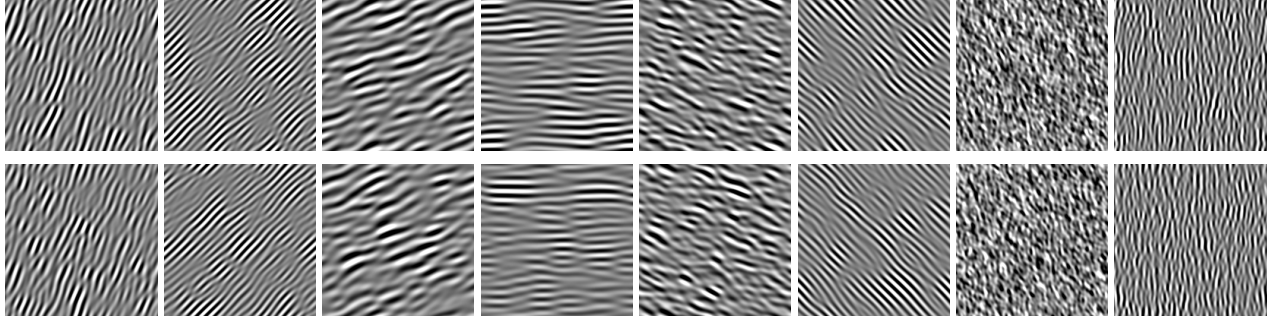


Figure 1: Uniform (top) vs. Bernoulli (bottom) weighting texture instances. The Poisson point distribution is used here with the cos kernel. No visual artifacts are introduced by the Bernoulli weighting. The same quality target is used for both alternatives, with $N = 30$ for uniform weighting and $N = 15$ for Bernoulli weighting.

3. Evaluation

3.1. Global process Gaussianity

Gabor noise is a process that converges in law: increasing the impulse density results in a process which is closer to the target Gaussian texture (*i.e.* random phases and a given target PSD). This in turn generates instances with the target appearance properties. However, a given instance of that process will not converge toward an asymptotic image: as more splats are added the texture pattern in the image will keep evolving forever, see fig. 2.

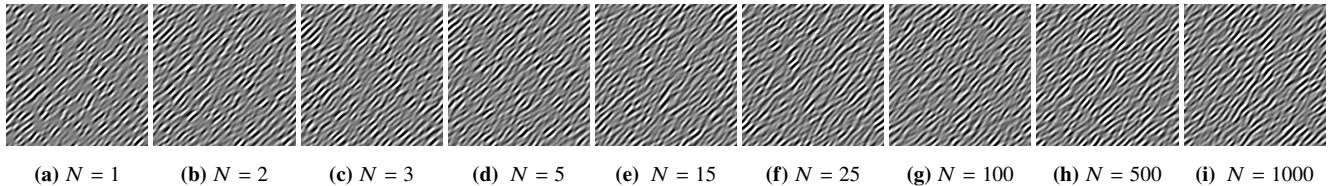


Figure 2: Process convergence of a given Gabor noise instance. Note how the first images are not Gaussian textures and won't reproduce the PSD — they show flat void regions and isolated ridges regions — then get reasonably converged at $N = 5$ (d), then have the pattern evolve forever as N increases ((e) to (i)), even though the target appearance (*i.e.* a Gaussian texture with the target PSD) is achieved.

We evaluate the global process Gaussianity as the Cramer von Mises (CvM) criterion [Wik18] of the noise process compared to the expected normal distribution. Formally, let $F_{n(\mathbf{x})}$ be the empirical distribution function of the noise process $n(\mathbf{x})$ and F^* the cumulative distribution function of the corresponding normal distribution with the same mean and standard deviation as the noise process. The Cramer von Mises criterion is then defined as:

$$CvM = \int_{-\infty}^{\infty} \left(F_{n(\mathbf{x})}(x) - F^*(x) \right)^2 dF^*(x)$$

This criterion is particularly suited for tests involving a large number of samples. It is also robust because it compares the entire support of the distribution instead of simple statistical moments. The effects of the proposed alternatives on the value of the CvM criterion are detailed in fig. 3.

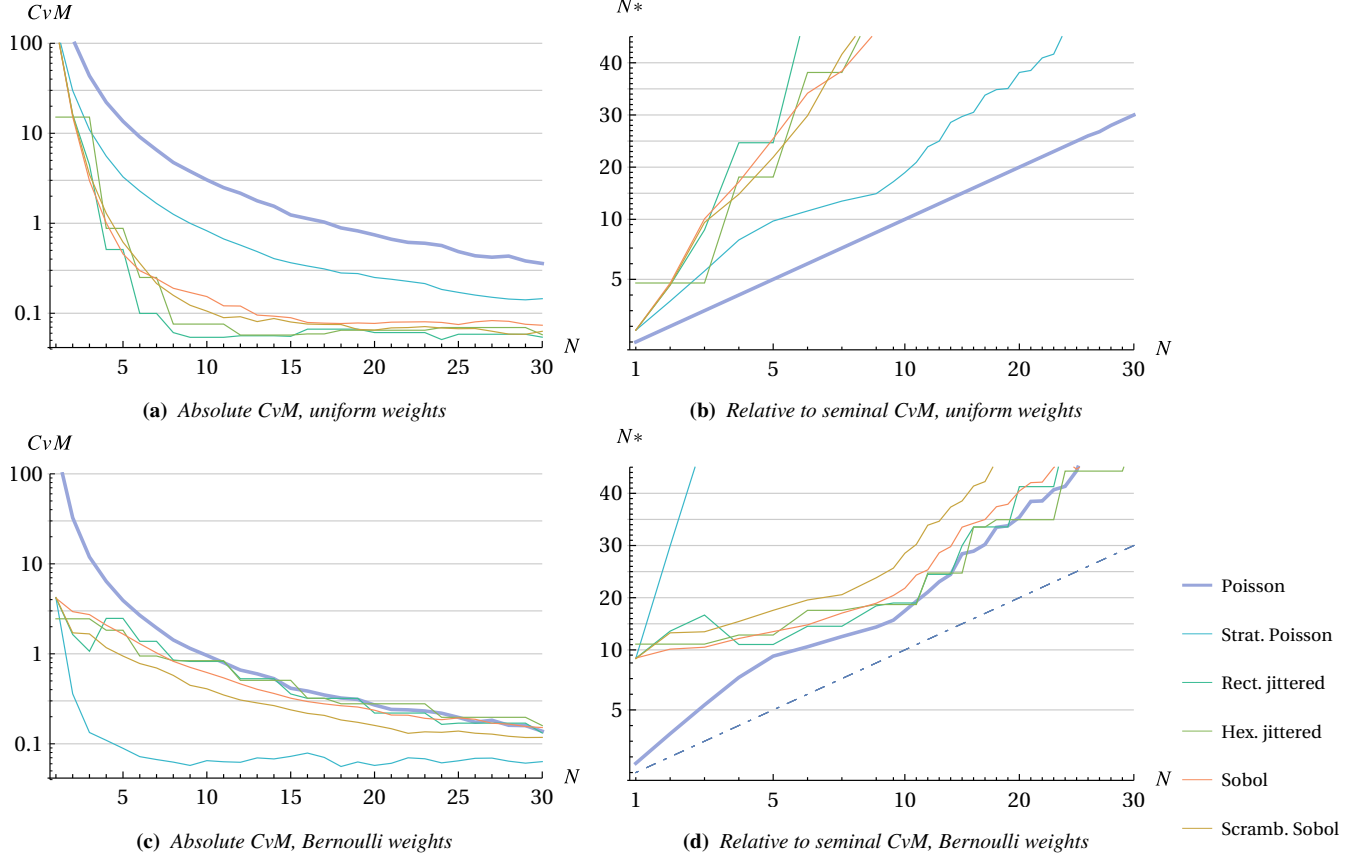


Figure 3: Effect of the alternative point distributions and random weights on the process convergence of Gabor noise. The CvM criterion is used to measure the distance between the noise process distribution and the normal distribution. The top row (a), (b) uses uniform weights in $[-1, 1]$ while the bottom row (c), (d) uses Bernoulli weights in $\{-1, 1\}$. The relative plots ((b), (d)) are obtained by using the absolute CvM value for the seminal approach as a reference: N^* is the impulse count of the seminal approach required to achieve the same CvM criterion as the alternative approach with an impulse count N . For each set of alternative elements, for every N , we evaluate a vector of 7 million Gabor noise samples obtained with independent sets of seeds, then we apply the CvM metric on the resulting vector.

3.2. Process at a given location

In the paper we show that the alternative Gabor Noise ingredients we benched did not impact stationarity even when the point distribution has a spatial bias. Here we show a more exotic plausible configuration for which it is not the case: using the sin kernel instead of cos, with no weighting at all (since this kernel is already of null mean).

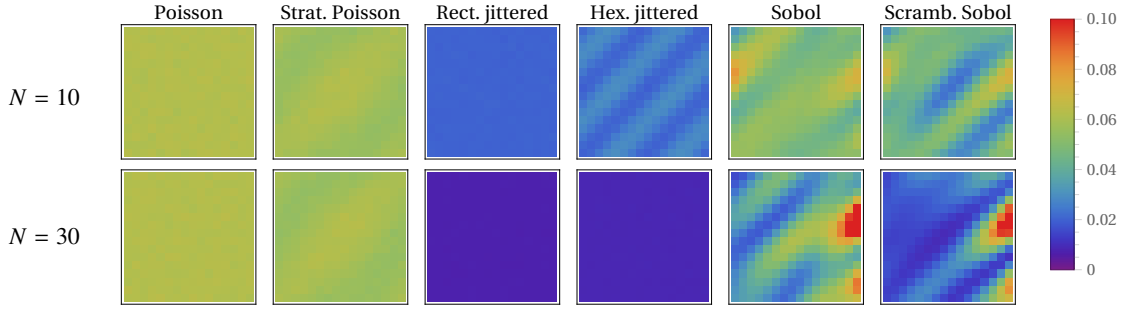


Figure 4: Variance of the Gabor noise process for each point in a cell, without weights and using the sin kernel (for a given F_0 and ω_0). In the absence of weights, all proposed alternatives exhibit unwanted spatial variations of the variance, most notably Sobol point distributions (rightmost two columns). Moreover, the variance evolves with N (top row vs. bottom row), which prevents any a priori normalization. Here, every point in each plot is obtained by computing the variance in the vector resulting from extracting the corresponding position within 16384 3×3 instances.

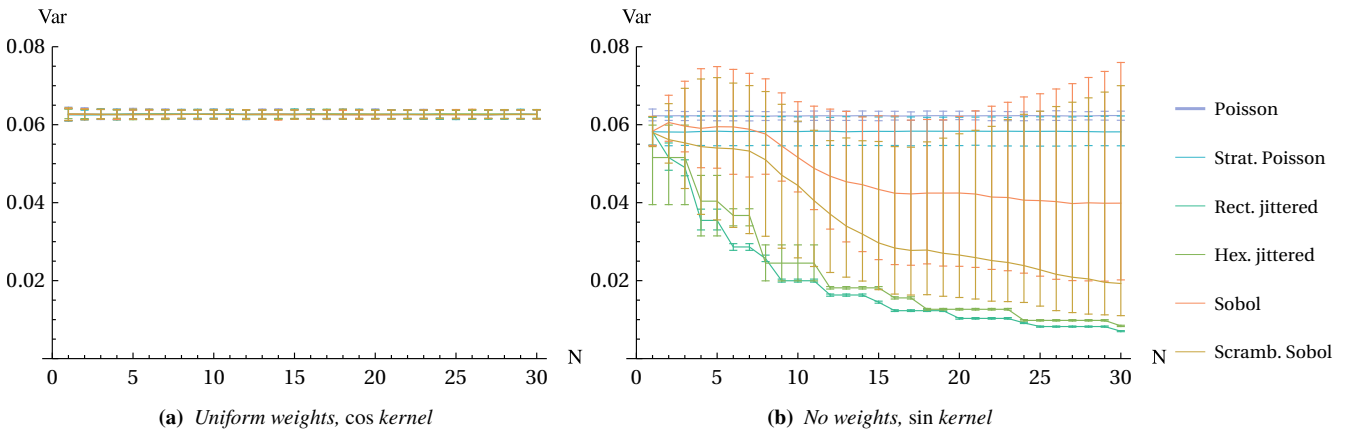


Figure 5: Variance of the process at given locations summarized by its median over a cell, for the proposed approaches. The error bars represent the 1st and 9th deciles compared to the median (solid line). The use of weights results in unbiased approaches (a) which have a constant variance with low variation around its median. Removing weights biases the approach because it breaks the translation invariance (i.e. stationarity over space, resulting in large error bars) and independence from N of the resulting process (as shown by the median varying with N) (b).

3.3. Instance stationarity and normalization

Here, we detail in figure 6 the plots about stationarity and normalization in instances, and in figure 7 a non-working case (the weighting-less approaches).

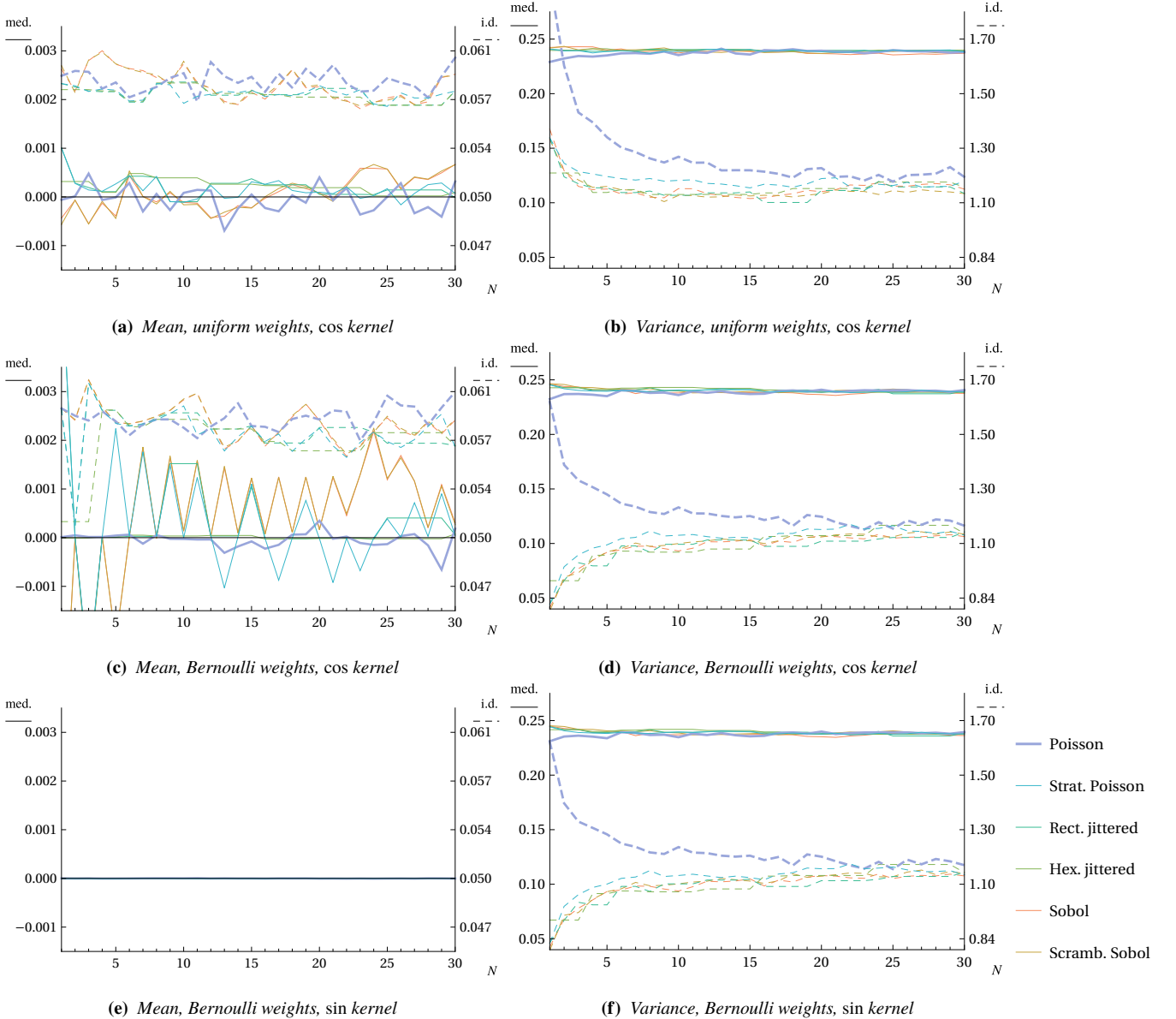


Figure 6: Fluctuation analysis of windowed average and contrast over instances of the proposed approaches. For each plot, for each N , 5000 instance images of 3×3 cells are generated and their image mean (resp. variance) are computed. We want to characterize the fluctuation in the obtained vector of 5000 values. Since this vector is not normally distributed, the mean and variance are not good descriptors of fluctuation. Instead, we study the median (solid lines) and interdecile range (dashed lines) of these samples, which are distribution-independent statistics.

Mean plots (left) show the absolute interdecile range $D_9 - D_1$, while variance plots (right) show the interdecile range relative to the median $(D_9 - D_1)/D_5$. The variations of the average (left) are small compared to the texture value range $[-1, 1]$, and null in the case of the sin kernel (e). The variations of the variance (right) are smaller for the proposed approaches compared to the seminal Gabor noise, i.e. they converge faster to the limit interdecile range for $N \rightarrow \infty$. This reveals that not only alternative approaches do provide reasonably stationary and directly normalized instances, but also that they are more stationary than the seminal approach over varying instances, as well as inside the whole image above cell size (due to the noise process ergodicity).

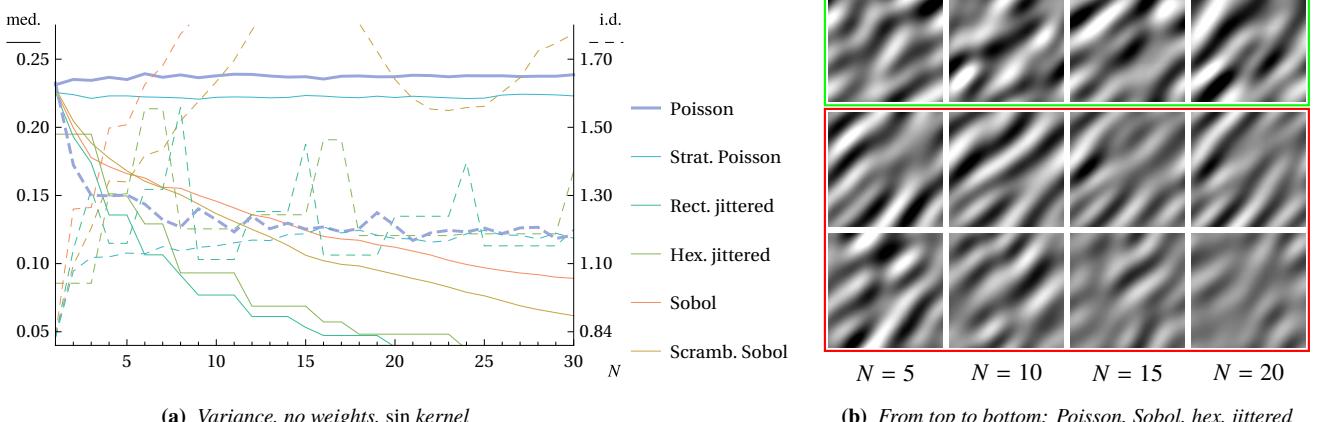


Figure 7: Fluctuation analysis of windowed contrast over instances of the broken approach described in section 3.2 (sin kernel with no weighting). Previously benched cases on spatially biased point distributions had no artifacts due to other Gabor noise ingredients restoring stationarity in the final result. The windowed variance is not stable when increasing N , and its interdecile range does not converge to a stable value. Furthermore, the instance variance value deviates from the process variance (e.g. for strat. Poisson) which makes a priori normalization of instances impossible. This bias is noticeable when looking at the contrast of generated instances for increasing N (b). We can interpret this as using uncorrelated null-mean random weights being the element that breaks the effects of correlation in point distributions.

References

- [CBEM05] CHI H., BEERLI P., EVANS D. W., MASCAGNI M.: On the Scrambled Sobol Sequence.
- [Sob67] SOBOL' I. M.: On the distribution of points in a cube and the approximate evaluation of integrals. *USSR Computational Mathematics and Mathematical Physics* 7, 4 (Jan. 1967).
- [Wik18] WIKIPEDIA: Cramér–von Mises criterion, 2018. Page Version ID: 864338045.